



Emerging role of wetland methane emissions in driving 21st century climate change

Zhen Zhang^{a,b,c,1}, Niklaus E. Zimmermann^{a,d}, Andrea Stenke^d, Xin Li^{c,e}, Elke L. Hodson^f, Gaofeng Zhu^g, Chunlin Huang^c, and Benjamin Poulter^{c,h}

^aDynamic Macroecology, Swiss Federal Research Institute WSL, Birmensdorf 8903, Switzerland; ^bInstitute on Ecosystems and Department of Ecology, Montana State University, Bozeman, MT 59717; ^cNorthwest Institute of Eco-Environment and Resources, Chinese Academy of Sciences, Lanzhou 730000, China; ^dDepartment of Environmental System Science, ETH Zürich, Zürich 8092, Switzerland; ^eCAS Center for Excellence in Tibetan Plateau Earth Sciences, Chinese Academy of Sciences, Beijing 100101, China; ^fOffice of Energy Policy and Systems Analysis, US Department of Energy, Washington, DC 20585; ^gKey Laboratory of Western China's Environmental Systems, Lanzhou University, Lanzhou 730000, China; and ^hBiospheric Sciences Laboratory, NASA Goddard Space Flight Center, Greenbelt, MD 20770

Edited by Wolfgang Lucht, Potsdam Institute of Climate Impact Research, Potsdam, Germany, and accepted by Editorial Board Member Hans J. Schellnhuber July 26, 2017 (received for review November 12, 2016)

Wetland methane (CH₄) emissions are the largest natural source in the global CH₄ budget, contributing to roughly one third of total natural and anthropogenic emissions. As the second most important anthropogenic greenhouse gas in the atmosphere after CO₂, CH₄ is strongly associated with climate feedbacks. However, due to the paucity of data, wetland CH₄ feedbacks were not fully assessed in the Intergovernmental Panel on Climate Change Fifth Assessment Report. The degree to which future expansion of wetlands and CH₄ emissions will evolve and consequently drive climate feedbacks is thus a question of major concern. Here we present an ensemble estimate of wetland CH₄ emissions driven by 38 general circulation models for the 21st century. We find that climate change-induced increases in boreal wetland extent and temperature-driven increases in tropical CH₄ emissions will dominate anthropogenic CH₄ emissions by 38 to 56% toward the end of the 21st century under the Representative Concentration Pathway (RCP2.6). Depending on scenarios, wetland CH₄ feedbacks translate to an increase in additional global mean radiative forcing of 0.04 W·m⁻² to 0.19 W·m⁻² by the end of the 21st century. Under the “worst-case” RCP8.5 scenario, with no climate mitigation, boreal CH₄ emissions are enhanced by 18.05 Tg to 41.69 Tg, due to thawing of inundated areas during the cold season (December to May) and rising temperature, while tropical CH₄ emissions accelerate with a total increment of 48.36 Tg to 87.37 Tg by 2099. Our results suggest that climate mitigation policies must consider mitigation of wetland CH₄ feedbacks to maintain average global warming below 2 °C.

global warming potential | climate feedbacks | inundation | radiative forcing | climate mitigation

Terrestrial wetlands are among the largest biogenic sources of methane contributing to growing atmospheric CH₄ concentrations (1) and are, in turn, highly sensitive to climate change (2). However, radiative feedbacks from wetland CH₄ emissions were not considered in the Coupled Model Intercomparison Project Phase 5 (CMIP5), and Integrated Assessment Models (IAM) assumed anthropogenic sources to be the only driver responsible for the increase of atmospheric CH₄ burden since the 1750s (3). The role of wetland CH₄ emissions, however, may play an increasingly larger role in future atmospheric growth of methane because of the large stocks of mineral and organic carbon stored under anaerobic conditions in both boreal and tropical regions. Paleoclimatological and contemporary observations of the climate sensitivity of wetland methane emissions suggest the potential for a large feedback (4), but there remains large uncertainty in quantifying the actual range of the response (5, 6).

Increasing air temperature is linked to the thawing of permafrost and to increased rates of soil microbial activity (7), which directly lead to greater CH₄ production in soils due to thaw-induced change in surface wetland areas (8). In the tropics, wetland areal extent is also influenced by precipitation, which affects the area of

surface inundation, water table depth, and soil moisture that, in turn, promote methanogenesis. Elevated CO₂ concentrations can increase ecosystem water use efficiency and thus soil moisture, and also increase soil carbon substrate availability for microbial activities (9). Tropical wetlands, for which a decline in inundation was observed in recent decades (10), are already exposed to increasing frequencies in extreme climate events, e.g., heat waves, floods, and droughts, and changes in rainfall distribution (11) and variability in methane emissions (12). Meanwhile, northern high-latitude ecosystems are experiencing a more rapid temperature increase than elsewhere globally and with increased rates of soil respiration (13), yet, locally at least, no response in methane emissions (14). Despite the importance of these feedbacks noted by the Intergovernmental Panel on Climate Change Fifth Assessment Report (IPCC AR5) (15), a comprehensive assessment of long-term global CH₄ feedbacks from changing wetland CH₄ emissions is still lacking.

To address uncertainties related to climate–wetland CH₄ feedbacks, we simulated an ensemble of wetland CH₄ emissions for the 21st century, and then quantified the wetland CH₄ contribution to radiative forcing (RF). Global mean air temperature change was estimated using the reduced complexity carbon cycle and climate model Model for the Assessment of Greenhouse-Gas Induced Climate Change Version 6 (MAGICC6) (16) and a

Significance

Conventional greenhouse gas mitigation policies ignore the role of global wetlands in emitting methane (CH₄) from feedbacks associated with changing climate. Here we investigate wetland feedbacks and whether, and to what degree, wetlands will exceed anthropogenic 21st century CH₄ emissions using an ensemble of climate projections and a biogeochemical methane model with dynamic wetland area and permafrost. Our results reveal an emerging contribution of global wetland CH₄ emissions due to processes mainly related to the sensitivity of methane emissions to temperature and changing global wetland area. We highlight that climate-change and wetland CH₄ feedbacks to radiative forcing are an important component of climate change and should be represented in policies aiming to mitigate global warming below 2°C.

Author contributions: Z.Z. and B.P. designed research; Z.Z., N.E.Z., X.L., and B.P. performed research; Z.Z., N.E.Z., A.S., E.L.H., G.Z., and C.H. contributed new reagents/analytic tools; Z.Z., G.Z., and C.H. analyzed data; and Z.Z., N.E.Z., A.S., X.L., E.L.H., and B.P. wrote the paper.

The authors declare no conflict of interest.

This article is a PNAS Direct Submission. W.L. is a guest editor invited by the Editorial Board.

¹To whom correspondence should be addressed. Email: yuisheng@gmail.com.

This article contains supporting information online at www.pnas.org/lookup/suppl/doi:10.1073/pnas.1618765114/-DCSupplemental.

sustained pulse–response model (17). A state-of-the-art land surface model, Lund–Potsdam–Jena Dynamic Global Vegetation Model (LPJ-DGVM) Wald Schnee und Landschaft version (LPJ-wsl), was used to quantify terrestrial wetland CH₄ emissions, in which permafrost and wetland area distribution and dynamics were estimated prognostically (18). Simulated global CH₄ emissions, calibrated such as to minimize the discrepancy between contemporary global annual CH₄ emissions, were estimated as a function of substrate, soil temperature, and soil moisture (19). Statistically representative estimates of mean and variance of future CH₄ emissions outputs were generated from 112 climate projections originating from 38 climate models of the CMIP5 ensemble (SI Appendix, Table S1) covering four Representative Concentration Pathway (RCP) storylines (20).

Materials and Methods

Wetland Definition. Wetlands are defined here as the land area that is either permanently or seasonally saturated, excluding small ponds, lakes, and coastal wetlands. Permanent wetlands comprise three general types: mineral wetlands (swamps and marshes), peatlands (permafrost, bog, fens), and seasonally flooded shallow water (floodplains). The methane-producing area is thus linked to inundation and freeze–thaw dynamics, which change geographically and temporally in response to soil water dynamics.

Model Description. The LPJ-wsl model is a process-based dynamic global vegetation model developed for carbon cycle applications based on development of the LPJ-DGVM (21). LPJ-wsl includes land surface processes, such as water and carbon fluxes, as well as vegetation demography and dynamics that are represented by plant functional types (PFTs) (22). The distribution of PFTs is simulated based on a set of bioclimatic limits and by plant-specific parameters that govern their physiological behavior and their competition for resources. Soil hydrology is modeled using a two-layer bucket model for hydrology and is coupled to an eight-layer freeze–thaw scheme and one-layer snow model to determine permafrost extent and ice content (23, 24) (SI Appendix, Methods).

Wetland area and dynamics were simulated following a modified version of the topography-based hydrological model (TOPMODEL) using a prescribed high-resolution topographic index based on a mapping product, hydrological data and maps based on shuttle elevation derivatives at multiple scales (HydroSHEDS) (25). HydroSHEDS was shown to agree most closely with observed wetland area in a comparison with existing global elevation datasets and parameterization schemes (18). Our TOPMODEL approach was optimized by calibrating parameters to match observations from a hybrid wetland area dataset (26) and a regional remote sensing surface inundation dataset (27).

We modeled net wetland CH₄ emissions to the atmosphere restricted to land areas where anaerobic soil conditions create low redox potentials required for methanogenesis. Net CH₄ emissions are estimated daily by combining wetland area (*A*) within a grid cell (*x*) with two soil temperature- and moisture-dependent scaling factors (*r*_{CH₄:C} and *f*_{ecosys}) applied to heterotrophic respiration (*R_h*),

$$E(x, t) = r_{\text{CH}_4:\text{C}} \cdot f_{\text{ecosys}}(x) \cdot A(x, t) \cdot R_h(x, t), \quad [1]$$

where *E*(*x*, *t*) is the net wetland CH₄ flux, *r*_{CH₄:C} is a fixed ratio of soil C to CH₄ emissions, and *f*_{ecosys} is a modifier that varies the CH₄ emission intensity for different biomes, which is optimized to match average annual emissions from an atmospheric inversion model (28). This approach thus estimates net methane emissions directly, and indirectly accounts for the individual processes of production and consumption of methane, and the various transport processes from the soil to the atmosphere. The comparisons of global and regional net CH₄ emissions between LPJ-wsl and other biogeochemical models are listed in SI Appendix, Table S2.

RF Calculations. Two methodologies for calculating RF were used to quantify the climate feedback from additional changes in CH₄ emissions from wetlands. The first method uses the carbon cycle climate model MAGICC6 (16), and the second method uses an emission-driven sustained pulse–response model (17), both relative to a reference year 1765. Because of the challenge to isolate the effect of anthropogenic forcing from wetland forcing in MAGICC6, the simple sustained pulse–response model was used to assess the impact of wetlands on RF by using prescribed anthropogenic sources since 1765 and adding the estimated total wetland emissions from LPJ-wsl. Before 1961, wetland CH₄ emissions were generated, following a uniform distribution,

by randomly selecting emissions from 1961 to 1990 to bring the RF value into equilibrium.

In MAGICC6, the lifetime of tropospheric methane is calculated by integrating the effects of hydroxyl radicals (OH) with the temperature-based chemical reaction rates. The observed CH₄ concentration changes over time are more accurately quantified by the net result of variations in emissions of multiple chemical compounds that affect the OH chemical sink, such as ozone, nitrogen oxides, carbon monoxide, and volatile organic compounds. In addition, the net atmospheric lifetime of CH₄ is determined by lifetimes of tropospheric OH, upland soil uptake, and the stratospheric losses. We prescribed the wetland CH₄ concentrations and corresponding anthropogenic CH₄ emissions for each RCP from IPCC AR5 (20).

In contrast, the sustained pulse–response model applies the perturbation lifetime of methane, which is designed to describe the overall long-term RF from CH₄ reactions with OH in the atmosphere (e.g., water vapor in stratosphere), as a constant value of 12.4 y (15). The instantaneous RF from CH₄ contributions at year *t* since the reference year *t'*, here the year 1765, is given by

$$\text{RF}_{\text{CH}_4}(t) = \xi_{\text{CH}_4} A_{\text{CH}_4} \int_0^t \Phi(t') e^{-(t-t')/\tau} dt', \quad [2]$$

where ξ_{CH_4} is a multiplier for CH₄ set to be 1.3; *A*_{CH₄} is the greenhouse-gas radiative efficiency ($1.3 \times 10^{-13} \text{ W}\cdot\text{m}^{-2}\cdot\text{kg}^{-1}$); and τ_i is the fixed perturbation lifetime for CH₄ (12.4 y). $\Phi(t)$ is a first-order decay function representing the lifetime of an individual net input of CH₄ into the background atmosphere according to IPCC 2013 (15),

$$\Phi(t) = r_0 e^{-t/\tau}, \quad [3]$$

where *r*₀ is the initial perturbation, and τ is the perturbation lifetime of CH₄. To estimate RF of equal mass of CO₂ in the atmosphere, five CO₂ decay pools with different fractions *f_i* (26%, 24%, 19%, 14%, and 18%) and adjustment times τ_i (3.4 y, 21 y, 71 y, 421 y, and 10⁸ y) are applied to describe the more complicated behavior of CO₂ (17). Thus the total CO₂ RF is given by

$$\text{RF}_{\text{CO}_2}(t) = \sum_{i=0}^4 \varepsilon_i A_i f_i \int_0^t \Phi_i(t') e^{-(t-t')/\tau_i} dt'. \quad [4]$$

To quantify the global warming effect of wetland and anthropogenic CH₄ sources, we used a modified metric Sustained Global Warming Potential (SGWP) [unit: kilograms CO₂-equivalents per year (kg CO₂-eq·y⁻¹)] (29) to evaluate the total cumulative RF effect from a persistent individual CH₄ source, which was defined as the sum of the time-integrated total RF (unit: watts per square meter), from Eqs. 2 and 4, over a given time horizon due to a sustained pulse emission of annual CH₄ emission (unit: teragrams) relative to a sustained pulse emission of an equal mass of CO₂ under present-day background conditions. This equation is given by

$$\text{SGWP}_{\text{CH}_4}(H) = \frac{\sum_0^H \text{RF}_{\text{CH}_4}(t) dt}{\sum_0^H \text{RF}_{\text{CO}_2}(t) dt}, \quad [5]$$

where *H* represents a certain time horizon. The SGWP for wetland and anthropogenic emissions was calculated with an initial year of 1765.

To quantify the total global warming contribution of wetland CH₄ emissions compared with anthropogenic counterpart, a Wetland Dominance Index (WDI) (unit: percent) was defined using following equation:

$$\text{WDI} = \left(\frac{\text{SGWP}_{\text{wetland}}}{\text{SGWP}_{\text{anth}}} - 1 \right) \times 100, \quad [6]$$

where SGWP_{anth} represents SGWP caused by anthropogenic activities.

Input Data and Model Experiments. As input to LPJ-wsl, the simulated meteorology, air temperature, total precipitation, and cloud cover from each of the CMIP5 models available from the Earth System Grid Federation was spatially downscaled and bias-corrected to match the spatial resolution (0.5°) and historical period of overlap (1960–1990) from Climatic Research Unit Time Series (CRU TS) Version 3.2.2. We conducted two sets of simulations for each of the climate projections, (i) a single spin-up simulation for 1,000 y with randomly selected, detrended 1961–1990 climate, and a constant atmospheric CO₂ concentration of 303 ppm by volume (the average for 1961–1990) and (ii) a combined historical and future simulation with time-varying CO₂ and climate data as defined by the corresponding RCP (20).

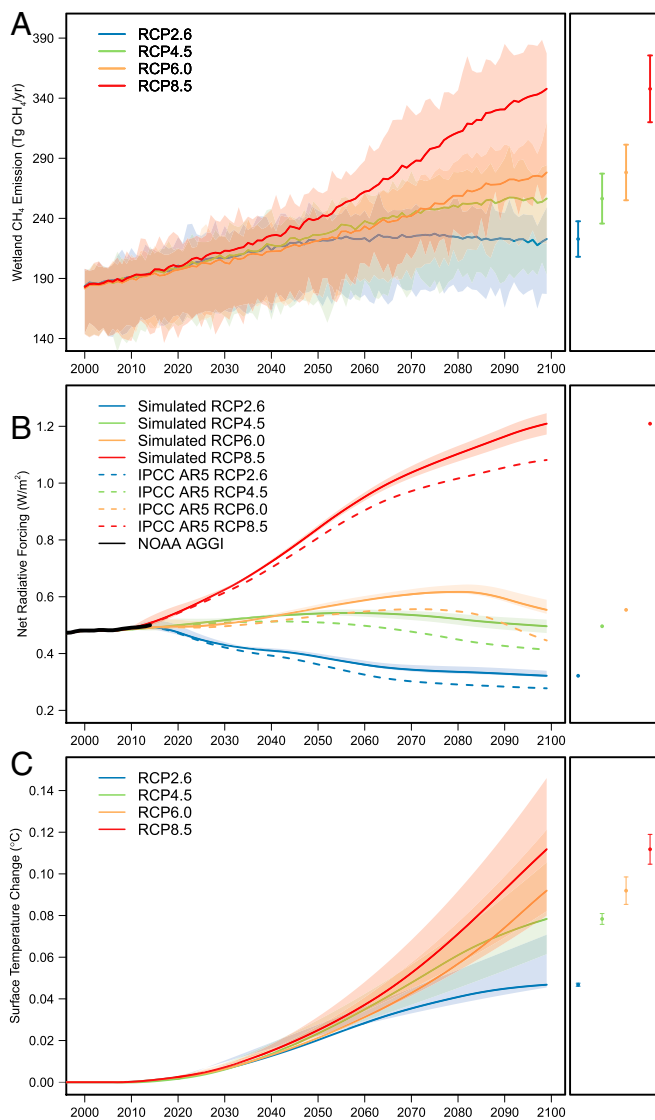


Fig. 1. Simulated future wetland CH₄ emissions, net RF, and net increase in global mean temperature using the simple carbon cycle climate model MAGICC6. Colored lines represent ensemble average estimates from using CMIP5 model outputs, and shaded areas represent the upper and lower range of estimates (Left). Mean and one-SD at the end of the 21st century (mean over AD 2099) for each metric are given by the bars (Right). (A) Simulated wetland CH₄ emissions driven by CMIP5 datasets for four RCPs. (B) Net RF from anthropogenic emissions with consideration of wetland CH₄ emissions feedback (solid lines) calculated by MAGICC6 and original projected RCPs without wetland CH₄ feedback (dashed lines) in IPCC AR5 and CMIP5, as well as observed RF (black solid line) based on atmospheric measurement from National Oceanic and Atmospheric Administration (NOAA) Annual Greenhouse Gas Index (AGGI). (C) Change in global mean temperature caused by wetland CH₄ feedback from MAGICC6 model.

Uncertainty Analysis. A statistical emulation of LPJ-wsl was parameterized to quantify model structural uncertainty and evaluate how it affected the simulated CH₄ fluxes. We adapted the multiple regression approach from ref. 30 and applied this within a Monte Carlo (MC) analysis to estimate the distribution of CH₄ emissions for each simulation. Parameters in the statistical model were fitted for each RCP. We assumed the parameters of the statistical model followed a normal distribution and used a 2D Latin Hypercube Sampling algorithm to generate 10,000 sets of parameters for each climate projection (SI Appendix, Fig. S7). We then conducted MC simulations with Eq. 1, for a total of 40,000 calculations, to derive the range of CH₄ emissions for each RCP (SI Appendix, Fig. S8). These ranges were only applied in MAGICC6 and the

simple sustained pulse-response model, to include the impact of model structural uncertainty on RF and SGWP calculations.

Results and Discussion

Mean global annual CH₄ emissions from natural wetlands were projected to increase from 172 Tg CH₄·y⁻¹ (1σ SD, ±12 Tg CH₄·y⁻¹) at present to 221.6 ± 15, 255 ± 20, 272 ± 21, and 338 ± 28 Tg CH₄·y⁻¹ in RCP2.6, RCP4.5, RCP6.0, and RCP8.5, respectively, by 2100 (Fig. 1A). In the strong climate mitigation scenario (RCP2.6), which includes the possibility of reaching the policy-relevant 2 °C target, wetland CH₄ emissions peak around the 2050s, with an average of ~225 Tg CH₄·y⁻¹, and decline thereafter. In contrast, RCP4.5 reveals wetland CH₄ emissions to increase to ~246 ± 21 Tg CH₄·y⁻¹ before the 2070s and then keep constant, with slightly lower emissions than the RCP6.0 scenario. In the “business-as-usual” scenario, RCP8.5, wetland CH₄ emissions roughly double by the 2090s relative to present-day emissions, with an increasing trend throughout the century. Based on the MAGICC6 approach, we find a 21st century wetland CH₄ RF feedback ranging from the 0.04 ± 0.002 W·m⁻² in RCP2.6, to 0.08 ± 0.003 W·m⁻² in RCP4.5, to 0.11 ± 0.004 W·m⁻² in RCP6.0, to 0.19 ± 0.01 W·m⁻² in RCP8.5 (Fig. 1B). These CH₄ RFs estimated by MAGICC6 are equivalent to 0.04 ± 0.001 °C, 0.07 ± 0.004 °C, 0.08 ± 0.006 °C, and 0.12 ± 0.01 °C increases in global mean temperature (Fig. 1C) under RCP2.6, RCP4.5, RCP6.0 and RCP8.5, respectively. Compared with the anthropogenic CH₄ emissions, wetlands account for 14.6 to 25.1% of the total projected RF change.

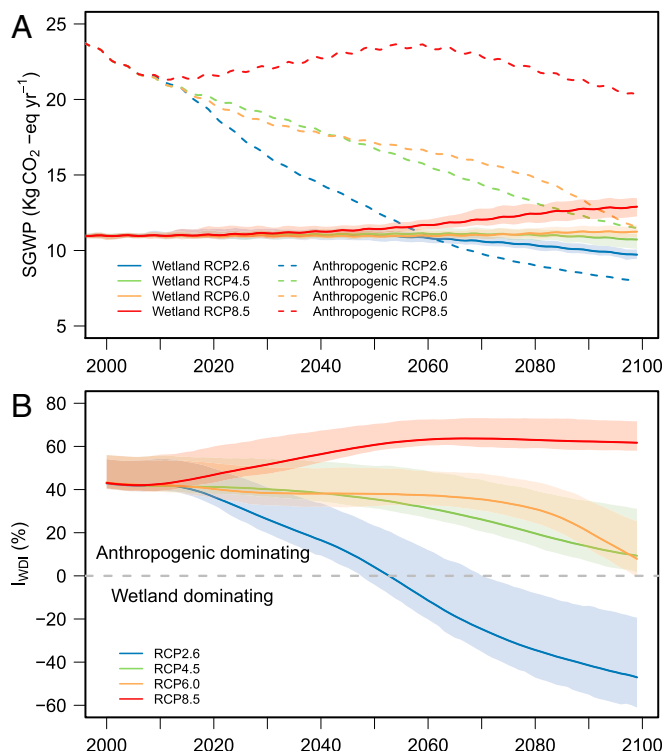


Fig. 2. Evolving pattern of wetland and anthropogenic CH₄ C change over varying time horizon since 1765 using simple sustained pulse-response model. (A) Time series of SGWP for wetland and anthropogenic CH₄ emissions. (B) Comparison of RF dominance between wetland and anthropogenic emissions. Here RF dominance is defined as a ratio of SGWP from wetlands to SGWP from anthropogenic sources. Shaded areas represent the upper and lower range of wetland estimates. Here the SGWPs from wetland and anthropogenic emissions were calculated as integrated RF of CH₄ since pre-industrial time (1765).

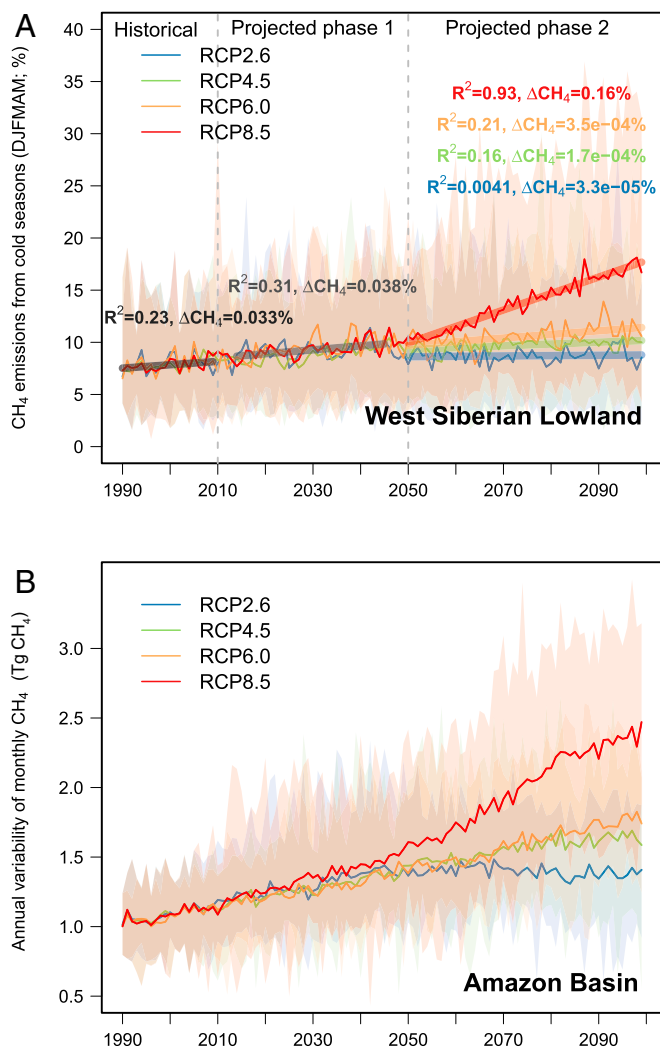


Fig. 3. Regional changes in wetland area extent and CH₄ emissions. (A) Contribution of CH₄ emissions from cold seasons (December to May) in boreal wetlands in WSL. Thick lines correspond to linear regression fits of ensemble anomalies. ΔCH_4 represents increasing contribution of CH₄ emission from cold seasons as percentage. (B) Annual variability in CH₄ emissions for the Amazon basin, which is defined as SDs of CH₄ fluxes within a year.

The ensemble estimates of SGWP demonstrate the possibility that wetlands overwhelm anthropogenic CH₄ emissions in driving future climate impacts under RCP26 (Fig. 2B). The wetland SGWP remains relatively constant at equilibrium state, and then varies with climate scenario (9.7 ± 0.3 kg CO₂-eq.y⁻¹, 10.7 ± 0.3 kg CO₂-eq.y⁻¹, 11.2 ± 0.4 kg CO₂-eq.y⁻¹, and 12.9 ± 0.7 kg CO₂-eq.y⁻¹ at the end of the 21st century for RCP26, RCP45, RCP60, and RCP85, respectively) (Fig. 2A). The constant SGWP represents an equilibrium state of the global methane budget before 1765, as assumed by IAM whereby chemical sinks balance most of natural emissions. The WDI exhibited large variation driven by RCP scenario, for example, for RCP2.6, natural wetlands clearly play a dominant role by the end of the 21st century, with WDI of $-47 \pm 9\%$. In contrast, the WDI kept a relatively constant value ($55 \pm 8\%$) since the 2050s under RCP8.5, suggesting that climate impact by wetlands is just half of the effect relative to increased anthropogenic emissions. Additionally, the climate feedback parameter, λ , from wetlands CH₄ is $\sim 0.03 \pm 0.001$ W·m⁻²·K⁻¹ under RCP85 (SI Appendix, Fig. S6), which falls within the range of previous estimates (2) and is approximately one tenth

of the surface albedo feedback from melting snow and ice cover (31).

Changes in 21st century wetland CH₄ emissions are strongly linked to the climate response wetland area extent and seasonality, which showed a diverse response across biomes (SI Appendix, Fig. S1). Ignoring potential human modification of wetlands, e.g., peatland drainage, the mean annual maximum global wetland area is expected to be 13% larger ($\sim 0.72 \pm 0.19$ Mkm²) in the 2090s for RCP8.5 scenario (SI Appendix, Fig. S2), whereas earlier studies have assumed no significant change in wetland area (32). Regionally, reduced precipitation causes a small decrease ($\sim 0.06 \pm 0.01$ Mkm² for RCP85) in tropical wetland area, whereas thawing of the near-surface permafrost stimulates a large increase ($\sim 0.58 \pm 0.15$ M·km² for RCP85) in boreal wetland area. However, despite decreasing tropical wetland extent and increased frequency of tropical drought, tropical wetlands remain the world's largest

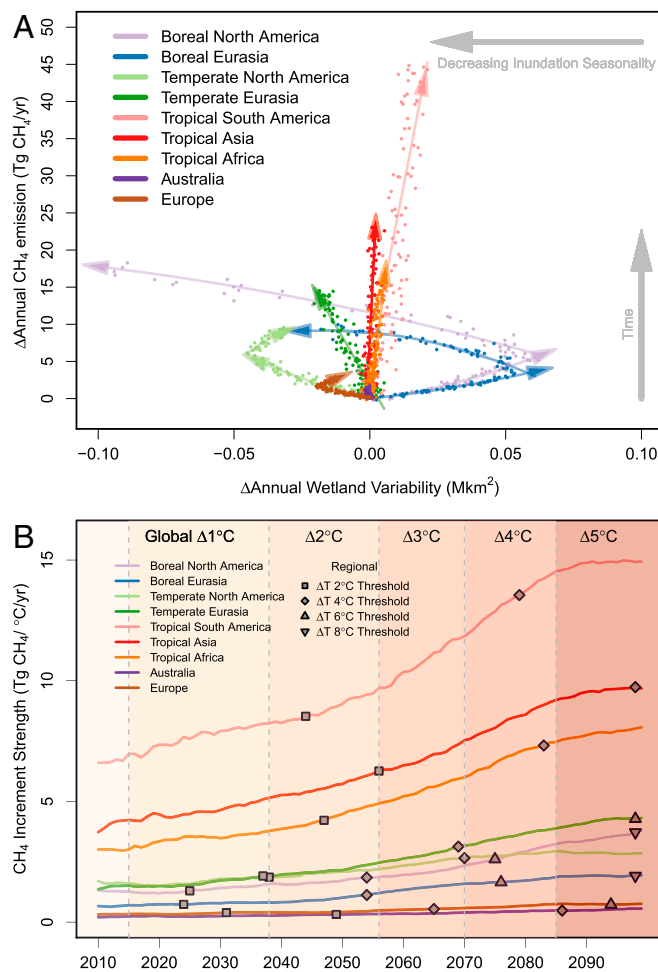


Fig. 4. Role of regional wetlands in changing wetland status and CH₄ emissions. (A) Scatterplot shows relationship between ensemble anomalies of annual wetland variability and anomalies of annual CH₄ emissions relative to 1960–1990 average levels for regional wetlands under RCP8.5. The linear least square regression fits represent the evolving trajectories of CH₄ emissions with increasing CH₄ emissions. The horizontal arrow represents the direction of increasing wetland CH₄ emissions with shifting patterns of inundation seasonality. The vertical arrow represents the evolving directions of both CH₄ emissions and inundation seasonality with time. (B) Increment of CH₄ emissions with rising temperature for regional wetlands. Background colors represent increases of global temperature from ensemble estimate of CMIP5 models under RCP8.5. Dots indicate regional increase of temperature at certain time. Details of calculation are provided in SI Appendix, Methods.

natural source responsible for $\sim 53.2 \pm 0.7\%$ by the end of the 21st century in RCP8.5. The annual contribution of boreal wetlands increases by $\sim 3.6 \pm 0.5\%$ from the present to the end of the 21st century, indicating higher sensitivity to climate change-driven CH₄ emissions in boreal regions because of thawing permafrost.

The increase in methane-producing wetlands in boreal regions was due primarily to increased near-surface soil moisture following permafrost thaw. More than half of global wetland area is positively correlated with air temperature while $\sim 40\%$ is negatively correlated (*SI Appendix, Fig. S3*). For instance, the West Siberian Lowland (WSL), one of the largest boreal wetlands, comprising $\sim 12.9\%$ of the global peatland area, exhibits an increase in CH₄ emissions during the transition from winter to spring, i.e., December to May (*SI Appendix, Fig. S4*). This originates from an increase in the thaw period and from higher heterotrophic respiration induced by higher soil temperatures. Projected thawing of permafrost and associated wetland expansion will largely affect CH₄ emissions from the taiga forest region in the WSL. From around the mid-2040s, a strong linear increase ($R^2 = 0.93, P < 0.01$) of CH₄ emissions with time, at a rate of 0.16% per year from winter to spring seasons, will occur under RCP8.5, despite environmental conditions changing more slowly in the WSL ($R^2 < 0.21, P > 0.01$) under all scenarios (Fig. 3A).

Long-term simulated tropical CH₄ emission changes are mainly associated with a shift in precipitation patterns. The partial correlation between global CH₄ emissions and climatic variables shows that spatial variation of CH₄ emissions is associated mainly with precipitation, and that this is especially important in tropical regions where the annual cycle of wet to dry seasons varies considerably. Consistent with an observed increase in the dry season in Amazonia since 1979 (11), our ensemble estimates predict a slightly negative trend in the basin-wide annual areal maximum of Amazonian wetlands by $\sim 4\%$ by the 2090s under RCP8.5. Despite there being no significant change in the proportion of CH₄ emissions from dry seasons across all RCP scenarios, we did find a steady increase in annual variability of CH₄ emissions (Fig. 3B).

We found a statistically significant relationship between seasonal wetland area variability and the increase in annual CH₄ emissions, despite diverse mechanisms driving large-scale CH₄ emission changes among wetlands (Fig. 4A). In addition, we show that seasonality of wetland area is an indicator for monitoring the long-term dynamics of CH₄ emissions at continental scale. Altered patterns in the trend of wetland variability coincide with the onset of a strong linear increase in CH₄ emissions in boreal wetlands, which suggests that CH₄ emissions are largely increased during cold seasons (December to February, March to May) afterward (*SI Appendix, Fig. S5*). The net growth rate of CH₄ emissions from the summer to autumn seasons is larger than that from the winter to spring seasons after the 2040s. In addition, the growth rates measured by regression lines among all regions characterize the strength of emitting CH₄ among major regions, where tropical wetlands show higher contributions than the other regions.

Our CH₄ RF estimates are subject to considerable uncertainties associated with estimation of natural sources and the resulting climate feedback. The representation of processes in LPJ-wsl assumes no effect of shifting spatial pattern of vascular plants on CH₄ transport from soil into atmosphere, which could lead to an underestimation of CH₄ emissions. Furthermore, microbial community composition might play an important role in driving CH₄ fluxes, but the biogeographical distribution of methanogen communities and their metabolic processes at ecosystem-scale are poorly understood due to the lack of observational data. In addition, uncertainties in RF estimates are also associated with the parameter values of the CH₄ lifetime and variations of global chemical CH₄ sinks, e.g., OH concentrations. To better understand the evolution of atmospheric CH₄ concentrations in the future, comprehensive in situ and remote sensing monitoring of CH₄ emissions and changes in wetland area are required.

The potential sensitivity of wetland CH₄ emissions to rising temperature highlights the need for limiting global warming below the 2 °C target. Climate-driven CH₄ emission feedbacks were positive for each wetland region (Fig. 4B), with large variability related to the different sensitivities of methanogenesis, freeze–thaw dynamics, and surface inundation. The timing of feedbacks was also variable, with increases in tropical wetlands emissions appearing to have a fairly abrupt response once global mean temperature approached 2 °C warming, whereas boreal wetlands, especially boreal North America, had more gradual increases in emissions due to expanding wetland area (33). Taking into account these additional changes in RF caused by increasing wetland CH₄ emissions emphasizes the need to consider wetland CH₄ feedbacks in IAM and to develop comprehensive greenhouse gas mitigation strategies. In addition, policy-relevant temperature targets must continue to incorporate assessments of feedbacks from terrestrial and oceanic systems for both CO₂ and non-CO₂ gases, like methane and nitrous oxide. With atmospheric methane concentrations now tracking the more fossil fuel-intensive scenarios (34), further insight into the climate sensitivity of methane sources and their chemical sinks remains of high importance.

ACKNOWLEDGMENTS. We thank Benjamin D. Stocker, Thomas Peter, Joeri Rogelj, and Leonardo Calle for constructive comments on the manuscript. We also thank Wolfgang Lucht and the anonymous reviewers for their detailed comments on the manuscript. We acknowledge the World Climate Research Programme's Working Group on Coupled Modeling, which is responsible for CMIP, and we thank the climate modeling groups for producing and making available their model outputs. Computational efforts were performed on the Hyalite High-Performance Computing System, operated and supported by Montana State University Information Technology Research Cyberinfrastructure. This study was funded by the Competence Center Environment and Sustainability (CCES) Project Modeling and Experiments on Land-Surface Interactions with Atmospheric Chemistry and Climate Phase 2 (MAIOLICA2) 42-01, Chinese Academy of Sciences (CAS) Project Big Earth Data Engineering, and the National Natural Science Foundation of China (Grants T411391001 and 91425303). This paper does not reflect the official views or policies of the United States Government or any agency thereof, including the Department of Energy.

- Tian H, et al. (2016) The terrestrial biosphere as a net source of greenhouse gases to the atmosphere. *Nature* 531:225–228.
- Arneeth A, et al. (2010) Terrestrial biogeochemical feedbacks in the climate system. *Nat Geosci* 3:525–532.
- Taylor KE, Stouffer RJ, Meehl GA (2011) An overview of CMIP5 and the experiment design. *Bull Am Meteorol Soc* 93:485–498.
- Hopcroft PO, Valdes PJ, O'Connor FM, Kaplan JO, Beerling DJ (2017) Understanding the glacial methane cycle. *Nat Commun* 8:14383.
- Schaefer H, et al. (2016) A 21st-century shift from fossil-fuel to biogenic methane emissions indicated by ¹³CH₄. *Science* 352:80–84.
- Nisbet EG, et al. (2016) Rising atmospheric methane: 2007–2014 growth and isotopic shift. *Global Biogeochem Cycles* 30:1356–1370.
- Yvon-Durocher G, et al. (2014) Methane fluxes show consistent temperature dependence across microbial to ecosystem scales. *Nature* 507:488–491.
- Cooper MDA, et al. (2017) Limited contribution of permafrost carbon to methane release from thawing peatlands. *Nat Clim Change* 7:507–511.
- van Groenigen KJ, Osenberg CW, Hungate BA (2011) Increased soil emissions of potent greenhouse gases under increased atmospheric CO₂. *Nature* 475:214–216.
- Prigent C, et al. (2012) Changes in land surface water dynamics since the 1990s and relation to population pressure. *Geophys Res Lett* 39:L08403.
- Fu R, et al. (2013) Increased dry-season length over southern Amazonia in recent decades and its implication for future climate projection. *Proc Natl Acad Sci USA* 110:18110–18115.
- Pandey S, et al. (2017) Enhanced methane emissions from tropical wetlands during the 2011 La Niña. *Sci Rep* 7:45759.
- Commane R, et al. (2017) Carbon dioxide sources from Alaska driven by increasing early winter respiration from Arctic tundra. *Proc Natl Acad Sci USA* 114:5361–5366.
- Sweeney C, et al. (2016) No significant increase in long-term CH₄ emissions on North Slope of Alaska despite significant increase in air temperature. *Geophys Res Lett* 43:6604–6611.
- Intergovernmental Panel on Climate Change (2013) *Climate Change 2013: The Physical Science Basis. Contribution of Working Group I to the Fifth Assessment*

Report of the Intergovernmental Panel on Climate Change (Cambridge Univ Press, Cambridge, UK).

16. Meinshausen M, Raper SCB, Wigley TML (2011) Emulating coupled atmosphere-ocean and carbon cycle models with a simpler model, MAGICC6 – Part 1: Model description and calibration. *Atmos Chem Phys* 11:1417–1456.
17. Frolking S, Roulet N, Fuglested J (2006) How northern peatlands influence the Earth's radiative budget: Sustained methane emission versus sustained carbon sequestration. *J Geophys Res Biogeosci* 111:G01008.
18. Zhang Z, Zimmermann NE, Kaplan JO, Poulter B (2016) Modeling spatiotemporal dynamics of global wetlands: Comprehensive evaluation of a new sub-grid TOP-MODEL parameterization and uncertainties. *Biogeosciences* 13:1387–1408.
19. Hodson EL, Poulter B, Zimmermann NE, Prigent C, Kaplan JO (2011) The El Niño–Southern Oscillation and wetland methane interannual variability. *Geophys Res Lett* 38:L08810.
20. Meinshausen M, et al. (2011) The RCP greenhouse gas concentrations and their extensions from 1765 to 2300. *Clim Change* 109:213–241.
21. Sitch S, et al. (2003) Evaluation of ecosystem dynamics, plant geography and terrestrial carbon cycling in the LPJ dynamic global vegetation model. *Global Change Biol* 9:161–185.
22. Poulter B, et al. (2011) Plant functional type mapping for earth system models. *Geosci Model Dev* 4:993–1010.
23. Gerten D, Schaphoff S, Haberlandt U, Lucht W, Sitch S (2004) Terrestrial vegetation and water balance—Hydrological evaluation of a dynamic global vegetation model. *J Hydrol (Amst)* 286:249–270.
24. Wania R, Ross I, Prentice IC (2009) Integrating peatlands and permafrost into a dynamic global vegetation model: 1. Evaluation and sensitivity of physical land surface processes. *Global Biogeochem Cycles* 23:GB3014.
25. Marthews TR, Dadson SJ, Lehner B, Abele S, Gedney N (2015) High-resolution global topographic index values for use in large-scale hydrological modelling. *Hydrol Earth Syst Sci* 19:91–104.
26. Poulter B, et al. (2016) Global wetland contribution to increasing atmospheric methane concentrations (2000–2012). *Environ Res Lett*, in press.
27. Hess L, et al. (2015) Wetlands of the lowland Amazon basin: Extent, vegetative cover, and dual-season inundated area as mapped with JERS-1 synthetic aperture radar. *Wetlands* 35:745–756.
28. Spahni R, et al. (2011) Constraining global methane emissions and uptake by ecosystems. *Biogeosciences* 8:1643–1665.
29. Neubauer S, Megonigal JP (2015) Moving beyond global warming potentials to quantify the climatic role of ecosystems. *Ecosystems (N Y)* 18:1000–1013.
30. Piao S, et al. (2013) Evaluation of terrestrial carbon cycle models for their response to climate variability and to CO₂ trends. *Global Change Biol* 19:2117–2132.
31. Soden BJ, Held IM (2006) An assessment of climate feedbacks in coupled ocean–atmosphere models. *J Clim* 19:3354–3360.
32. Stocker BD, et al. (2013) Multiple greenhouse-gas feedbacks from the land biosphere under future climate change scenarios. *Nat Clim Change* 3:666–672.
33. Serreze M, Francis J (2006) The Arctic amplification debate. *Clim Change* 76:241–264.
34. Saunio M, Jackson RB, Bousquet P, Poulter B, Canadell JG (2016) The growing role of methane in anthropogenic climate change. *Environ Res Lett* 11:120207.